

Heart Rate Measurement using an Earphone-Type Wearable Device Equipped with Biodegradable Piezoelectric Sensors

Keitaro Nonaka¹, Shumma Jomyo^{1,2}, Hideki Aiko³, Shuichi Tasaka³, Harutoyo Hirano⁴, and Toshio Tsuji¹

Abstract—In recent years, there has been increased interest in using wearable devices for continuous physiological monitoring, which has promising applications in personal health management and clinical practice. This study proposes a method for estimating heart rate using an earphone-type device equipped with a low-power, structurally simple piezoelectric sensor that captures pressure pulse wave signals in the external auditory canal. The proposed method applies two-stage noise removal filtering based on physiologically plausible R–R intervals (RRI) and signal amplitude components, enabling stable heart rate detection even under conditions with external disturbances. When applied to both resting and stimulating periods, the proposed method achieved an agreement rate exceeding 95% after noise removal and demonstrated a strong correlation with heart rate values obtained from ECG. Notably, motion and pain stimuli introduced noise into the signal during the stimulus periods; nevertheless, the proposed method effectively suppressed spurious peak detections arising from transient disturbances.

I. INTRODUCTION

In recent years, as population aging has advanced in developed countries, extending healthy life expectancy has emerged as a critical social challenge, accompanied by growing interest in disease prevention and daily health management. Routine measurement and monitoring of biological signals, such as heart rate, are effective means of detecting early-stage physiological abnormalities. This acquired data are expected to support personal health management and diagnostic support in medical settings.

Against this background, wearable devices that can be used to take prolonged measurements have become widespread as a means of continuously monitoring biosignals in daily life. Currently available commercial devices include wrist-worn devices capable of measuring heart rate and simple electrocardiograms [1], [2], as well as ring-type devices capable of measuring parameters such as heart rate and body temperature [3], [4]. However, since these devices are worn on peripheral sites such as the wrist or fingers, they are susceptible to motion artifacts and changes in posture. Moreover, reduced peripheral blood flow in cold

¹K. Nonaka, S. Jomyo and T. Tsuji are with the Graduate School of Advanced Science and Engineering, Hiroshima University, Higashi-Hiroshima, 739-8527, Japan keitarononaka@hiroshima-u.ac.jp

²S. Jomyo with Department of Electrical and Information Engineering, National Institute of Technology, Kure College, 2-2-11 Agaminami, Kure, Hiroshima, 737-8506, Japan

³H. Aiko and S. Tasaka are with Earfredo Co., Ltd., 2-3-12 Minamihonnmachi, Chuo-ku, Osaka, 541-0054, Japan

⁴H. Hirano is with Department of Medial Equipment Engineering, Clinical and Educational Collaboration Unit, School of Medical Sciences, Fujita Health University, 1-98 Dengakugakubo, kutsukake-cho, Toyoake, Aichi, 470-1101, Japan



Fig. 1: Earphone-type device.

environments leads to unstable perfusion [5], resulting in degraded measurement accuracy. To address these issues, ear-worn approaches for acquiring physiological information have recently drawn attention. Physiologically, the external auditory canal is supplied by the superficial temporal artery [6] and has a higher perfusion value than other peripheral sites [5], while being less susceptible to autonomic nervous system influences. These characteristics make the ear a promising measurement site for acquiring stable biological signals. Sensor systems have been proposed that measure blood oxygen saturation and heart rate at the earlobe using photoplethysmography (PPG) sensors [7]. Nevertheless, PPG sensors present structural and technical challenges: they require both a light source and a photodetector, leading to relatively high power consumption; they demand greater thickness and space for the sensor assembly; and they are prone to noise from skin-surface reflections and ambient light [8]. These drawbacks, especially power consumption, pose critical constraints for wearables intended for long-term continuous monitoring.

A non-optical, low-power piezoelectric film sensor, referred hereafter as 'Picoleaf', has been developed as an alternative to PPG sensors [9]. This Picoleaf can measure heart rate, respiration, and peripheral arterial stiffness [10], [11] and is designed with an ultrathin and highly flexible material, achieves excellent conformability to curved surfaces, ensuring comfort during wear. In addition, Picoleaf does not require an optical emitter and operates at a markedly lower power than optoelectronic PPG sensors. This study proposes a system that uses an earphone-type wearable device equipped with Picoleaf to measure auricular pressure pulse waveforms and estimate heart rate.

II. MATERIALS AND METHODS

A. Measuring instruments

We developed a prototype earphone-type device by combining a smart earphone (Earfredo Co., Ltd.) and Picoleaf

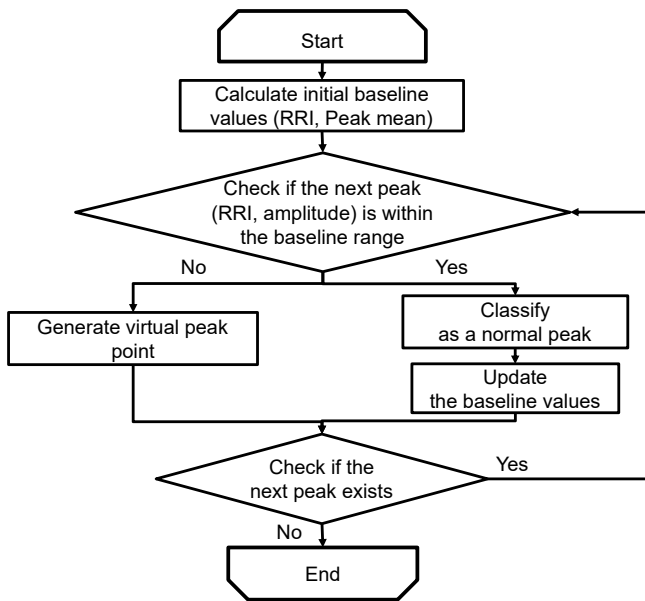


Fig. 2: Flowchart of the noise removal algorithm.

(Fig. 1). The device incorporates Picoleaf internally and is worn on the external auditory canal, allowing the sensor to closely adhere to the skin surface of the ear and continuously measure pulse waves in the external auditory canal.

Picoleaf converts resistance changes caused by physical deformation of the sensor, induced by pressure variations in the vascular walls due to cardiac pulsation, into electrical signals. This enables measurement of pulse waves containing biological information such as heart rate and R-R intervals (RRIs). The sensor consists of a piezoelectric film based on flexible polylactic acid (PLA), which exhibits excellent responsiveness to pressure variations. Owing to its large piezoelectric constant (5.8 pC/N) and low dielectric constant ($\epsilon = 2.7$ F/m), it enables more efficient conversion of pressure changes into electrical signals [9], [12]. Furthermore, PLA is a biodegradable polymer derived from lactic acid, which is produced by fermenting plant-based starch using lactic acid bacteria. It possesses the characteristic of being decomposable under natural environmental conditions after use. Consequently, PLA serves as a carbon-neutral material that reduces CO₂ emissions throughout its entire life cycle—from production and use to disposal and degradation [13]. The combination of environmental compatibility and high pressure sensitivity in such a biodegradable piezoelectric sensor represents a novel approach toward the development of sustainable wearable devices, distinguishing it from conventional non-biodegradable sensors.

B. Extract of heartbeats

We consider the calculation of heart rate from pulse wave signals measured at the external auditory canal. Since the pulse waveforms differ from electrocardiogram (ECG) signals in their characteristics, a peak detection algorithm for ECG signals [10] was modified to dynamically detect and remove outlier peaks in pulse waves obtained from Picoleaf.

Fig. 2 shows the processing steps of the algorithm. The algorithm exploits the periodicity of the pulse waveform to predict the location and interval of the next peak based on previously validated normal peak information. It also removes as noise any measurements that exhibit large discrepancies from these predictions. The algorithmic details are provided below:

- 1) **Calculation of initial averages:** For the first 11 peaks, calculate the average peak-to-peak intervals and amplitude (denoted RRI_{mean} and $Peak_{mean}$, respectively).
- 2) **Outlier detection:** For the next peak, determine whether the RRI and amplitude of the next peak exceed the allowable ranges of RRI_{mean} and $Peak_{mean}$.
- 3) **If within normal range:** Slide the peak window by one, update RRI_{mean} and $Peak_{mean}$ based on the latest 11 peaks, and repeat the process.
- 4) **If detected as noise:** Remove the peak and insert a “virtual peak” based on prior information. This virtual peak represents the expected peak position if noise had not occurred and serves as a reference for subsequent peak evaluations.
- 5) **Update upon confirmation of normal peaks:** After interpolation, once a normal peak is confirmed again, update RRI_{mean} and $Peak_{mean}$ and return to normal processing.

At the start of processing, a contiguous set of 11 peaks is extracted, and the averages of the peak intervals and amplitudes are computed. We only use beats whose RRI falls within the typical physiological range of 0.6–1.2 seconds to calculate initialization of these averages. This prevents outliers from affecting the initialization and preserves the accuracy of subsequent noise classification.

Outlier detection involves checking whether the RRI deviates by more than $\pm 30\%$ from RRI_{mean} and whether the amplitude deviates by more than $\pm 50\%$ from $Peak_{mean}$. These thresholds balance tolerance to physiological variability against effective noise removal. To maintain continuity in RRI even when peaks are erroneously removed as noise, the method introduces “virtual peaks”. These are assumed to exist at positions obtained by adding $Peak_{mean}$ to the previous normal peak location. By re-evaluating the RRI between virtual peaks and subsequent peaks, continuous assessment is possible, minimizing the impact of noise-induced peak loss on analysis accuracy. Employing 11 peaks provides a stable reference that avoids overreacting to transient beat-to-beat variability, while sliding-window updates allow the evaluation criteria to adapt progressively to the current physiological state.

III. EXPERIMENT

To verify the validity of the proposed heart rate estimation method, an electrical stimulation task was performed at varying stimulus intensities. The accuracy of heart rate estimation before and after noise removal procedure on external auditory canal pressure pulse signals, acquired using the earphone-type device described in Section II-A was compared. Ten healthy adult males (mean age: 22.25 ± 1.16

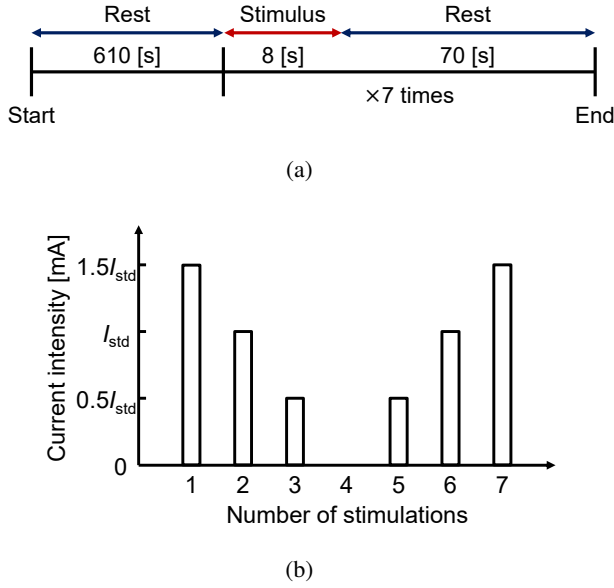


Fig. 3: Experimental configurations: (a) experimental protocol and (b) valley-type stimulus currents. I_{std} : standard current amplitude.

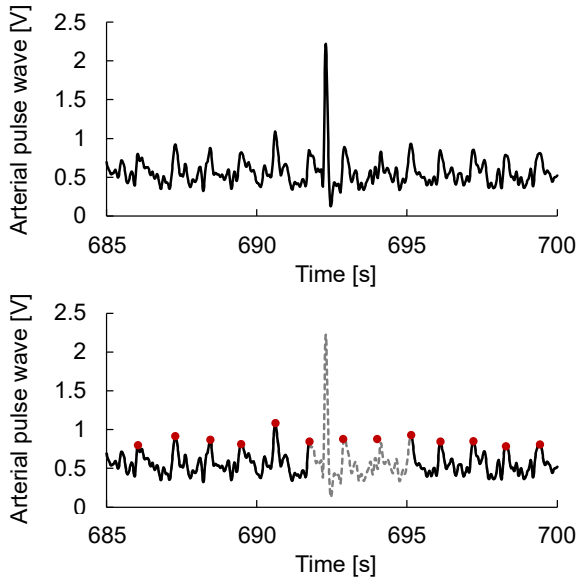


Fig. 4: An example of measured arterial pulse waveforms. (Top) Original waveform measured over 15 s. (Bottom) Denoised waveform with interpolated peaks, shown as red dots.

years) participated in this experiment. This experiment was performed in accordance with the Declaration of Helsinki and was approved by the Research Ethics Committee of the Graduate School of Advanced Science and Engineering, Hiroshima University (approval number: E2015-0017).

A. Experimental protocols

The experimental protocol is shown in Fig. 3(a). After a 610-second resting induction period to stabilize baseline biological recordings, seven trials of continuous stimulation tasks were conducted. Each trial consisted of an 8-second trial of continuous electrical stimulation, followed by a 40-second of resting period. This yielded 48 seconds per trial, giving a total experiment duration of 1,156 seconds. The stimulus intensity was defined with the baseline current corresponding to a numerical rating scale (NRS) pain score of 3 as 1.0 times. The stimulation intensities were presented in the following order as shown in Fig. 3(b): 1.5, 1.0, 0.5, 0, 0.5, 1.0, and 1.5 times the baseline current. Participants were placed in the supine position inside a dark room to minimize external influences during the experiment.

Both pulse wave and ECG signals were measured simultaneously in this experiment. The pulse wave was measured using the prototype earphone-type device described in Section II-A. ECG signals were recorded using a biological information monitor (BP-608EV, Omron Healthcare Co., Ltd.). All analog signals were digitized by an A/D converter (DC-300H, NIHON KOHDEN Corp.) at a sampling frequency of 10 kHz and stored on a PC. The electrical stimulation system consisted of an isolator (SS203J, NIHON KOHDEN Corp.), a function generator (WF1973, NF Corporation), and an electrical stimulator (SEN-3401, NIHON KOHDEN Corp.). A 250 Hz sinusoidal electrical stimulation was delivered to the participant's right forearm.

B. Analysis procedure

The effectiveness of the proposed noise processing algorithm was demonstrated by adopting accuracy (Acc) as the evaluation metric. Accuracy was defined based on the deviation between the reference and estimated values as given by Equation (1).

$$\text{Acc} = \left(1 - \frac{|\text{TP} - \text{EP}|}{\text{TP}} \right) \times 100, \quad (1)$$

where TP denotes heart rates obtained from the electrocardiography, and EP denotes heart rates measured by the proposed device.

The agreement rate between the heart rate obtained from the unprocessed waveform containing noise, before applying the proposed algorithm, and the heart rate obtained from the processed waveform was calculated. The heart rate estimation results based on the electrocardiogram were used as the true value. A paired t -test at a significance level of 5% was conducted to evaluate the difference in the agreement rates.

IV. RESULTS

Fig. 4 shows an example of the pulse wave signal used for analysis. The upper panel represents the raw waveform obtained from the sensor, while the lower panel shows the waveform after peak interpolation processing. The solid line indicates the waveform after noise removal, and the dashed line represents the original waveform containing peaks identified as noise. Red dots denote the interpolated peak points

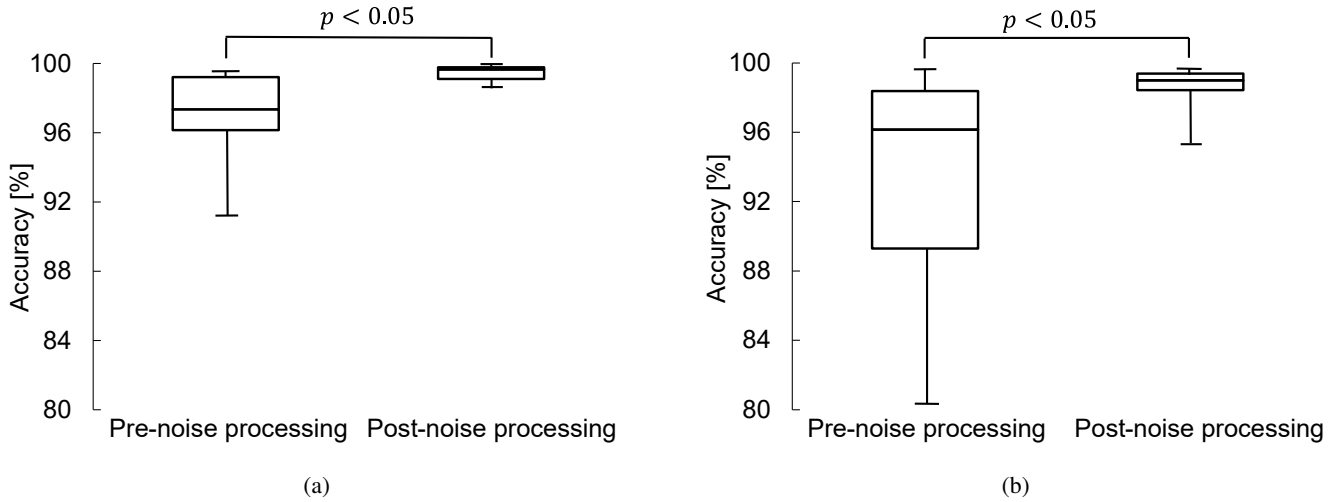


Fig. 5: Comparison of heart rate matching rates, calculated from both unprocessed and noise-processed waveforms: (a) resting period and (b) stimulating period.

estimated based on the proposed algorithm, which were subsequently used to calculate heart rate intervals and other analytical parameters.

Fig. 5(a) shows Acc of heart rate estimation during the resting period across all participants, before and after noise removal. Prior to noise removal, the minimum, median, and maximum Accs were 91.2%, 97.4%, and 99.6%, respectively; after noise removal, they improved to 98.6%, 99.7%, and 100%, respectively. Statistical analysis revealed significant differences in Accs before and after noise removal ($p < 0.05$). Fig. 5(b) shows heart rate Acc during the stimulating period across the participants, before and after noise removal. Prior to noise removal, the minimum, median, and maximum Accs were 80.3%, 96.6%, and 99.8%, respectively; after noise removal, they improved to 95.3%, 99.0%, and 100%, respectively. A significant difference between pre- and post-removal was observed ($p < 0.05$).

Fig. 6(a) shows the relationship between heart rates estimated from noise-processed pulse waves and those obtained from ECG during the resting period. These measures exhibited a strong correlation ($r = 0.999, p = 1.94 \times 10^{-12}$), suggesting that the proposed method enables highly accurate heart rate estimation during the resting period. Fig. 6(b) illustrates the relationship between heart rates estimated from noise-processed pulse waves and those obtained from ECG. During the stimulating period, the two measures showed a strong correlation ($r = 0.994, p = 7.67 \times 10^{-9}$), indicating that the proposed method can achieve high accuracy in heart rate estimation even under the stimulating period. Furthermore, the high estimation accuracy observed during the stimulating period was maintained at a level comparable to that during the resting period, demonstrating the robustness and general applicability of the proposed method. Fig. 7 presents the proportion of heartbeats removed by the noise processing algorithm throughout each period. During resting periods, the noise removal rate had a minimum, median, and maximum of 2.0%, 10.1%, and 28.8%, respectively.

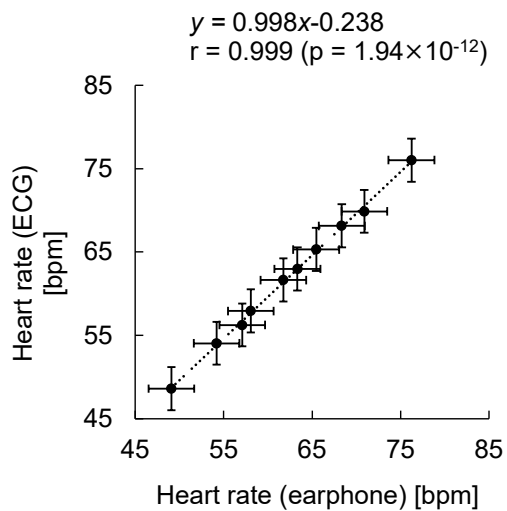
In contrast, during the stimulation period, those rates were 9.8%, 32.4%, and 55.1%, respectively.

V. DISCUSSION

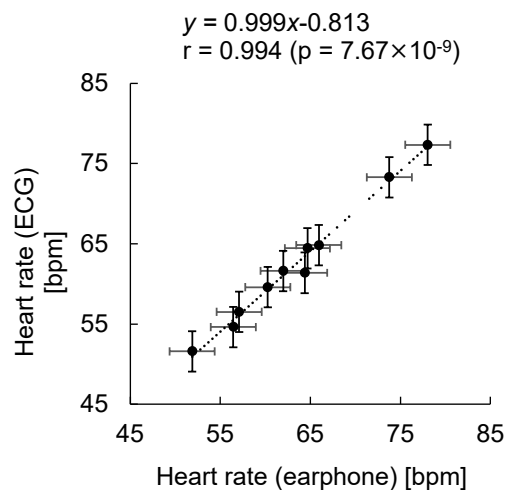
The post-denoising agreement rate for the pressure pulse wave signals measured by the earphone-type device exceeded 95% in both periods. These findings suggest that the proposed noise processing algorithm enables stable heart rate estimation even under transient disturbance conditions. In particular, disturbances caused by body movements or pain stimuli were expected to affect the output of the piezoelectric sensor during stimulus periods. The device used in this study is designed to be worn in the external auditory canal, and thus its performance may be influenced by individual differences and the stability of attachment. Nevertheless, the proposed noise removal algorithm, which combines RRI and amplitude components, effectively suppressed erroneous peak detections caused by short-term disturbances, thereby contributing to improved accuracy.

Furthermore, the analysis of the noise removal rate showed that the removal rate in the resting period was lower than that in the stimulating period, indicating that the quality of physiological signals is more stable under resting conditions. This finding suggests that data acquired during the resting period are more suitable for precise physiological signal evaluation and quantitative analysis. Conversely, the higher removal rate observed during the stimulating period reflects the frequency of motion artifacts and disturbances, implying that the removal rate itself could potentially be used as an indicator for motion detection or activity level assessment.

The applicability of the proposed method is particularly promising in clinical setting that requires long-term physiological monitoring, such as intensive care units and rehabilitation contexts. Continuous monitoring with a minimally obtrusive, earphone-type device has the potential to enable real-time vital sign monitoring while reducing participant burden.



(a)



(b)

Fig. 6: Comparison of heart rates obtained from a earphone-type sensor and an electrocardiograph: (a) resting period and (b) stimulating period.

On the other hand, the participants in this study were limited to healthy young males, which may pose a limitation in generalizing the proposed method. Previous studies have reported that in elderly individuals and patients with cardiovascular diseases, decreased vascular elasticity and altered hemodynamics can lead to reduced pulse wave amplitude and phase delay [14]. Therefore, for these populations, more robust signal processing techniques—such as enhanced noise removal and delay compensation—may be required. In addition, during the present experiment, some subjects exhibited a higher incidence of noise, suggesting that adaptive methods capable of dynamically adjusting processing parameters according to individual differences and fitting conditions should be explored in future work. In particular, the application of machine learning for feature extraction and noise estimation could further improve the robustness of

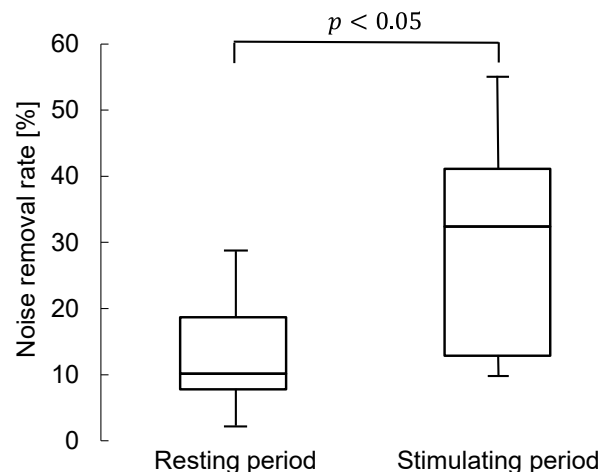


Fig. 7: Noise removal rate in resting and stimulating periods.

signal processing under diverse physiological conditions.

VI. CONCLUSIONS

This paper proposed a novel earphone-type device equipped with a biodegradable piezoelectric sensor incorporating a noise removal algorithm, and assesses the effect of this algorithm on the accuracy of heart rate estimation. The results showed the device achieved an agreement rate exceeding 95% in both the resting and the stimulating period, demonstrating improved estimation accuracy relative to conventional methods. These results suggest that the proposed method is effective even under conditions with strong noise influences caused by external disturbances or body movements. Furthermore, the findings confirmed that the proposed method enables continuous and reliable acquisition of physiological data using an earphone-type device, which is comfortable to wear in daily life.

As a future perspective, we plan to develop algorithms that enable simultaneous measurement of respiratory rate in addition to heart rate estimation. Furthermore, for applications involving elderly individuals or patients with cardiovascular diseases—where pulse wave propagation delay and signal degradation may occur—adaptive noise reduction and delay compensation using machine learning are required. In addition, by implementing wireless communication and real-time processing on edge devices, the proposed system is expected to evolve into a more practical physiological monitoring platform applicable to a wide range of situations, including clinical settings and home healthcare.

VII. ACKNOWLEDGEMENTS

This study was partly supported by the JSPS KAKENHI grant (22H00197). We are also grateful to the study volunteers for their participation.

REFERENCES

- [1] A. Shcherbina, C. M. Mattsson, D. Waggott, H. Salisbury, J. W. Christle, T. Hastie, M. T. Wheeler, and E. A. Ashley, "Accuracy in wrist-worn, sensor-based measurements of heart rate and energy

- expenditure in a diverse cohort,” *Journal of Personalized Medicine*, vol. 7, no. 2, 2017.
- [2] H. J. Saarinen, A. Joutsen, K. Korpi, T. Halkola, M. Nurmi, J. Herne-
nesniemi, and A. Vehkaoja, “Wrist-worn device combining ppg and
ecg can be reliably used for atrial fibrillation detection in an outpatient
setting,” *Frontiers in Cardiovascular Medicine*, vol. Volume 10 - 2023,
2023.
- [3] A. Maijala, H. Kinnunen, H. Koskimäki, T. Jämsä, and M. Kangas,
“Nocturnal finger skin temperature in menstrual cycle tracking: ambu-
latory pilot study using a wearable oura ring,” *BMC Women’s Health*,
vol. 19, no. 1, p. 150, 2019.
- [4] H. Kinnunen, A. Rantanen, T. Kenttä, and H. Koskimäki, “Feasible
assessment of recovery and cardiovascular health: accuracy of noctur-
nal hr and hrv assessed via ring ppg in comparison to medical grade
ecg,” *Physiological Measurement*, vol. 41, no. 4, p. 04NT01, 2020.
- [5] K. Budidha and P. A. Kyriacou, “The human ear canal: investigation
of its suitability for monitoring photoplethysmographs and arterial
oxygen saturation,” *Physiological Measurement*, vol. 35, no. 2, p. 111,
2014.
- [6] M. Masè, A. Micarelli, and G. Strapazzon, “Hearables: New perspec-
tives and pitfalls of in-ear devices for physiological monitoring, a
scoping review,” *Frontiers in Physiology*, vol. Volume 11 - 2020, 2020.
- [7] D. B. Ellebrecht, D. Gola, and M. Kaschwich, “Evaluation of a
wearable in-ear sensor for temperature and heart rate monitoring: A
pilot study,” *Journal of Medical Systems*, vol. 46, no. 12, p. 91, 2022.
- [8] K. B. Kim and H. J. Baek, “Photoplethysmography in wearable
devices: A comprehensive review of technological advances, current
challenges, and future directions,” *Electronics*, vol. 12, no. 13, 2023.
- [9] M. Ando, H. Kawamura, K. Kageyama, and Y. Tajitsu, “Film sensor
device fabricated by a piezoelectric poly(l-lactic acid) film,” *Japanese
Journal of Applied Physics*, vol. 51, no. 9S1, p. 09LD14, 2012.
- [10] Z. Xu, T. Sakagawa, A. Furui, S. Jomyo, M. Morita, M. Ando, and
T. Tsuji, “Toward a robust estimation of respiratory rate using car-
diovascular biomarkers: Robustness analysis under pain stimulation,”
IEEE Sensors Journal, vol. 22, no. 10, pp. 9904–9913, 2022.
- [11] Z. Xu, T. Sakagawa, A. Furui, S. Jomyo, M. Morita, M. Ando, and
T. Tsuji, “Beat-to-beat estimation of peripheral arterial stiffness from
local pwv for quantitative evaluation of sympathetic nervous system
activity,” *IEEE Transactions on Biomedical Engineering*, vol. 69,
no. 9, pp. 2806–2816, 2022.
- [12] E. J. Curry, K. Ke, M. T. Chorsi, K. S. Wrobel, A. N. Miller, A. Patel,
I. Kim, J. Feng, L. Yue, Q. Wu, C.-L. Kuo, K. W.-H. Lo, C. T.
Laurencin, H. Ilies, P. K. Purohit, and T. D. Nguyen, “Biodegradable
piezoelectric force sensor,” *Proceedings of the National Academy of
Sciences*, vol. 115, no. 5, pp. 909–914, 2018.
- [13] L. Murata Manufacturing Co., “Picoleaf product page,”
<https://www.murata.com/products/sensor/picoleaf>, accessed 31
July 2025.
- [14] G. F. Mitchell, “Arterial stiffness in aging: Does it have a place in
clinical practice?” *Hypertension*, vol. 77, no. 3, pp. 768–780, 2021.